Citation: R. I. Woodward and D. D. Hudson (2022). Mode-locked mid-infrared fiber systems. In S. Jackson, M. Bernier and R. Vallée (Eds.), Mid-Infrared Fiber Photonics, Woodhead Publishing.

DOI: 10.1016/B978-0-12-818017-4.00002-1

Chapter 11

Mode-Locked Mid-Infrared Fiber Systems

Robert I. Woodward and Darren D. Hudson

ABSTRACT

The generation of ultrashort optical pulses from laser technologies significantly broadens their range of applications. While near-IR ultrafast fibre lasers are now essential tools in science, industry and medicine, devices operating in the mid-IR are currently much less mature. Alongside the general challenges of extending fibre lasers to longer wavelengths, there are also numerous complications to the application of current mode-locking techniques to generate picosecond and femtosecond pulsed outputs in this spectral region. Fortunately, there has been significant progress in this field in recent years, leading to record performance and opening up new transformative applications. In this Chapter, we review the technical challenges and state-of-the-art in long-wavelength mode-locked fibre lasers, including consideration of pulse metrology, mid-IR modulation techniques and cavity designs, and soliton physics in soft glasses. By capitalising on these advances, recent works have demonstrated impressive mid-IR laser sources with few-cycle pulse durations, 10s kW peak powers and tunability over 100s nm. The future appears bright for mid-IR mode-locked fibre lasers and we conclude with a perspective on future work and routes to practical deployment.

KEYWORDS

mode-locking, ultrafast lasers, picosecond pulses, femtosecond pulses, pulse generation, dispersion, nonlinearity, solitons, saturable absorbers, mid-infrared, fibre lasers

11.1 INTRODUCTION

Since the early days of laser technology, it was realised that the generation of ultrashort *pulses* of light could significantly expand the space of applications served by coherent light sources. The development of mode-locking techniques—which establish a fixed phase relationship between the longitudinal modes of a laser cavity, producing pulses on picosecond and femtosecond timescales [1]—made this vision a reality, and ultrafast mode-locked lasers are now essential tools across science, industry and medicine.

This progress, however, is almost entirely based on near-IR mode-locked sources. There is thus vast potential for new transformative photonic technologies by pushing the wavelength of such devices into the mid-IR. For example,

by directly targeting absorption resonances of fundamental bonds in polyatomic molecules, many new laser processing opportunities are created. This includes cutting and micro-machining of materials such as polymers, through exploiting the C-H bond absorption features around 3–4 μm, in addition to targeting hydrocarbon bonds in tissues and proteins for new surgical procedures. Selective bond excitation also enables precise control of reaction pathways for the nascent field of mode-selective chemistry, which shows great promise for advancing the pharmaceutical industry but is currently limited in scale by a lack of suitable high-intensity light sources. Finally, ultrashort pulses of mid-IR light are also required as pump sources for nonlinear optical processes, which are both an active area of fundamental research and of practical importance, e.g. to drive octave-spanning supercontinua for broadband sensing (see Chapter 12).

With these exciting prospects, it is unsurprising that a number of ultrashort-pulse mid-IR laser architectures are actively being explored (for a comprehensive overview, see Refs [2, 3]). Firstly, building on the success of ultrafast near-IR sources, nonlinear parametric down-conversion schemes are currently the most advanced, e.g. optical parametric chirped pulse amplification (OPCPA), capable of generating microjoule-level few-optical-cycle pulses, with broad tunability [4]. The size and complexity of such systems is highly prohibitive to their practical deployment however, especially in resource-limited environments. Similarly, mode-locked bulk gain materials like chromium- and iron-doped II-VI chalcogenides offer emission from 2.0 to 3.5 μm and 3.5 to 5.5 μm, respectively, although are practically limited e.g. by requiring cryogenic cooling for iron-based lases [5]. Finally, QCLs have had major impact as a compact solution for CW to nanosecond mid-IR light emission, but their electron dynamics fundamentally prohibit femtosecond pulse generation. To overcome these limitations, recent research has therefore focused on rare-earth-doped *fibre* lasers.

Fibre laser technology already represents the fastest growing segment of the billion-dollar laser market, driven by the many benefits the platform provides for end-users: flexibility, compact footprint, high beam quality etc. *Mode-locked* fibre lasers are no exception, with near-IR ultrafast ytterbium-doped fibre lasers competing seriously with the current workhorse mode-locked titanium:sapphire systems. Could fibre lasers therefore be an ideal solution for mid-IR mode-locked source development?

This chapter addresses this question, considering both the state-of-the-art and the technical challenges in moving mode-locked fibre lasers from the near-IR to longer wavelengths. We note that our discussion is limited to passive mode-locking, since there have yet to be demonstrations of actively mode-locked (i.e. using electronically switched intensity or phase modulators) mid-IR fibre lasers, partly due to limited availability of such modulators for the mid-IR. Indeed, the lack of commercially available components and requirement to use novel non-standard materials (with very different properties to typical near-IR components) are the main challenges in this field. This can also be viewed as an opportunity, however, as the new parameter space of soft glass mid-IR materials opens up

new routes for both fundamental investigation and practical source development.

The first challenge we consider in Section 11.2 is the characterisation of ultrafast mid-IR lasers. Section 11.3 then provides a brief historical perspective of mode-locked mid-IR fibre source development, followed by a comprehensive survey of the current state of picosecond mid-IR fibre sources in Section 11.4, with an emphasis on saturable absorber-based techniques. Femtosecond lasers are considered in Section 11.5, including discussion of soliton effects and the impact of mid-IR glass properties on their performance. Finally, we evaluate the outstanding challenges and future prospects for the technology in Section 11.6.

11.2 MEASUREMENT TOOLS

Diagnostic tools operating in the near-IR offer affordable, sensitive, and accurate characterisation of laser pulses. These traits, combined with low cost and robust performance, have been a major driver in the ascension of near-IR ultrafast laser performance. Beyond 2 μm however, these tools offer poorer performance due to reductions in properties such as material transparency and photodetector band-gap mismatch. In this section, we review some of the necessary changes in tooling required to perform ultrafast pulse characterisation in the mid-IR wavelength range.

11.2.1 Photodetectors

High-speed photodetectors are standard tools in ultrafast laser laboratories as they provide an excellent way to find mode-locking regimes, diagnose the stability of the pulse train, and monitor for Q-switching instabilities. Semiconductor photodetection in the near-IR typically relies on the group IV systems of silicon and germanium or III-V systems typically based on InGaAsP. These systems offer high quantum-efficiency and high speed from the visible to the near-IR, but have severely reduced response beyond around 2 μm due to their large bandgap energy. To overcome this limitation, lower-energy (i.e. narrow) bandgap semiconductors must be employed such as the III-V system of Indium Antimonide (InAs), the IV-VI system of Lead Selenide/Sulfide (PbSe-S), and the II-VI system of Mercury Cadmium Telluride (HgCdTe). Photodiode response curves of various narrow-bandgap semiconductors are shown in Fig. 11.1. For an in-depth look at the physics of mid-IR photodetection the reader is referred to Ref. [6].

HgCdTe detectors currently offer the best performance for high-speed pulse measurement in the mid-IR. Commercial detectors (e.g. Vigo Systems, Thorlabs) can cover 2-10 μm with detection bandwidth of 100s of MHz, which is fast enough to resolve typical mode-locked pulse trains. It should be noted, however, that the native response of these detectors is typically $< 10^7$ cm $\cdot \sqrt{\text{Hz}}/\text{W}$ and thus at least one amplifier stage is required for practical pulse measurements. Active cooling of the photodiode can increase detectivity by more than one order of magnitude, although this comes at the cost of increased system complexity.

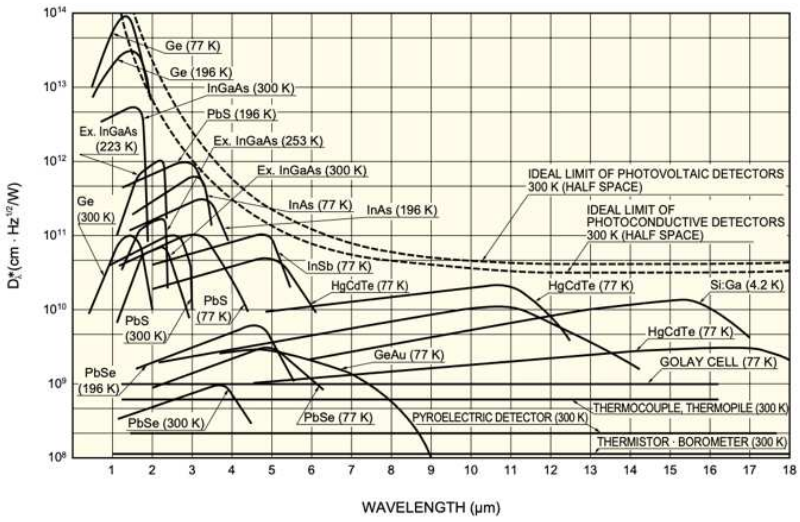

FIGURE 11.1 Response curves for various mid-IR photodetector technologies (after Ref. [7]).

11.2.2 Pulse Measurement

While the photodetection systems discussed in the previous section allow for characterizing the pulse train, they are typically far too slow to analyse individual ultrashort pulses. The techniques that have been demonstrated so far for this purpose in the mid-IR include 2-photon autocorrelation, second-harmonic generation (SHG) autocorrelation, and SHG-Frequency Resolved Optical Gating (FROG). While the topology of these systems is identical to near-IR versions, the second harmonic crystals and photodetectors are substantially different.

11.2.2.1 Autocorrelation

Perhaps the simplest mid-IR pulse measurement system is the 2-photon autocorrelator based on InGaAs. Standard InGaAs detectors are responsive from around 800 - 1700 nm, which in principle means they can be used in 2-photon autocorrelation systems from > 1700 nm to 3400 nm. As well, extended InGaAs photodetectors that offer response out to 2400 nm could extend the 2-photon autocorrelation range to 4800 nm. A typical setup is achieved with a standard Michelson interferometer using a pellicle beamsplitter to provide near 50/50 splitting and a computer-controlled stage to provide the variable delay. Several versions of these autocorrelators have been demonstrated with the main differences relating to the choices of beam-splitters, delay stage range, and interferometer type. By implementing a lock-in amplifier, significant gains can be achieved in SNR, allowing for measurement of low peak power pulses.

Another closely related method to measure pulses in the mid-IR is the SHG-

autocorrelator based on a mid-IR compatible second harmonic crystal. A range of crystals exist that can be effectively phase-matched, with the most common being $AgGaS_2$ (see following section). One advantage of SHG-autocorrelation is that a background-free pulse measurement is possible by using a cross-beam geometry, which simplifies the pulse analysis.

11.2.2.2 Frequency Resolved Optical Gating

FROG measurements provide the full electric field of the pulse and are widely considered to be the preferred method of ultrashort pulse measurement. At the heart of FROG is the spectrogram measurement, which is the spectrum of the second harmonic signal as a function of delay. Once the spectrogram is recorded, a retrieval algorithm can be used to work out the full pulse amplitude and phase [8].

Thus, the only changes required to create a mid-IR FROG versus a near-IR FROG are appropriately selecting the second harmonic crystal and using a spectrometer that works at the SHG wavelength. The first demonstration in this space used an $AgGaS_2$ crystal [9] for this purpose to record a FROG spectrogram of a sub-100 fs pulse at 3.2 μm (generated via OPCPA). In this experiment, the second harmonic signal at 1650 nm was spectrally analysed using a fast linear-array spectrometer based on InGaAs (rather than the usual silicon based linear arrays found in most FROGs).

In Ref. [9] it was shown that a range of crystals could be used for mid-IR FROGs, however $AgGaS_2$ was chosen due to its reasonably high nonlinear parameter (d_{eff} = 9.11 pm/V), wide transparency (0.5-13 μm), and environmental stability. The first measurement of a mid-IR fibre laser pulse via FROG was presented in Ref. [10], where the full amplitude and phase information showed a clear third-order dispersion on the laser pulse. This information helped confirm the hypothesis that the laser was operating in a soliton mode-locked state, which does not compensate for higher-order dispersion.

11.3 EARLY MODE-LOCKED MID-IR FIBRE LASERS

Efforts to generate ultrashort pulses from mid-IR fibre lasers can be traced as far back as 1996, when researchers inserted thin layers of indium arsenide (InAs) semiconductor exhibiting nonlinear (saturable) absorption into an Er:ZBLAN laser cavity [11]. Figure 11.2(a) shows the original cavity design, including 1.2 m multimode Er:ZBLAN fibre butt-coupled to two mirrors, with InAs layers on the output mirror, pumped with a 650 nm DCM dye laser. The system emitted an 84 MHz pulse train at 1 mW average power [Figure 11.2(b)–(c)]—an impressive result for the early stage of mid-IR fibre laser development—but limited diagnostics meant the pulse profile and optical spectrum were not measured (the use of long-pass filters confirmed operation on the 2.7 μm transition, however). Additionally, the pulse train exhibited strong Q-switching modulation, and thus, is more accurately described as Q-switched mode-locking.

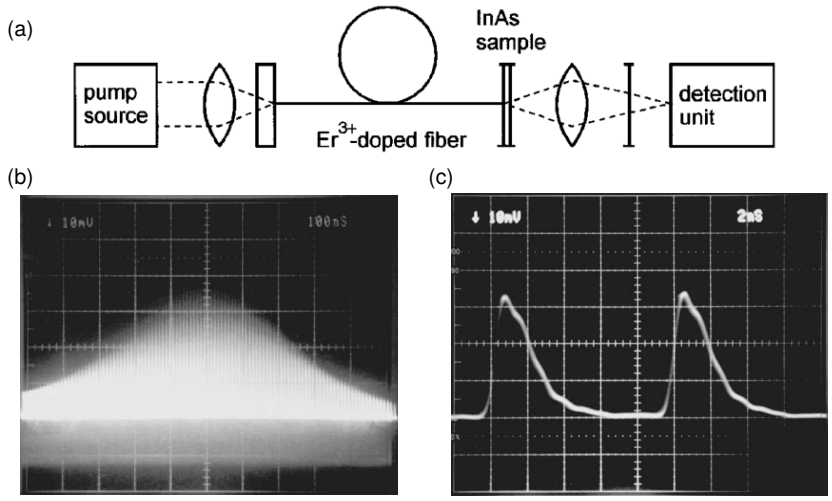

FIGURE 11.2 First reported mode-locked mid-IR fibre laser (after Ref. [11]): (a) cavity design; (b) mode-locked pulse train within Q-switched envelope (measured using photodiode-detection and an oscilloscope); (c) magnified region showing two mode-locked pulses.

Following this pioneering result, there was more than a decade of little reported progress. Fortunately, there has recently been a resurgence of investigation into mode-locked fibre lasers beyond 2.5 μm, with significant strides made towards practical systems to meet the needs of real-world applications. We note that the current reported sources can be broadly categorised as picosecond lasers, which to date have employed saturable absorber materials to achieve mode-locking, and femtosecond lasers, which have exploited nonlinear fibre optic effects for mode-locking. For clarity of discussion, we therefore treat each category separately and summarise the state of the art, alongside considering the practical challenges for each mode-locking technique that arises in the mid-IR region.

11.4 STATE OF THE ART: PICOSECOND SYSTEMS

In this section, we evaluate the state of the art in mode-locked mid-IR fibre lasers generating picosecond-duration pulses. Table 11.1 is a compilation of all published lasers meeting this criteria, to the best of our knowledge. Performance highlights and trends are now discussed, in the context of optimizing laser designs to continue advancing pulsed source performance in this space. It should be noted that the majority of lasers in this section employ saturable absorbers as the pulse generating mechanism; we thus begin with consideration of saturable absorber technology for the mid-IR.

Ion	Saturable Absorber	Wavelength (um)	Duration (ps)	Energy (nJ)	Peak Power (kW)	Year: Ref.
Er	SESAT			0.02		1996: [11]
	Fe:ZnSe	2.783		0.93		2012: [12]
	SESAM	2.797		8.50		2014: [13]
	SESAM	2.78	25	46.54	1.86	2015: [14]
	BP	2.783	42	25.50	0.61	2016: [15]
	Graphene	2.785	42	0.70	0.02	2016: [16]
	SESAM	2.71–2.82	6.4	7.02	0.97	2017: [17]
	BP	3.489				2018: [18]
Ho/Pr	SESAM	2.87	24	4.90	0.21	2012: [19]
	SESAT	2.86	6	2.78	0.47	2014: [20]
	BP	2.866	8.6	6.28	0.64	2016: [21]
	SESAM	2.84–2.88	22	12.56	0.50	2017: [22]
	Cd_3As_2	2.86	6.3			2017: [23]
	FSF	2.864	4.7	10.00	1.87	2019: [24]
Dy	FSF	2.97–3.30	33	2.70	0.08	2018: [25]

TABLE 11.1 State of the art in picosecond mode-locked mid-IR fibre lasers. Entries are left blank where the quantity was not measured / cannot be computed using the available data. SESAT: semiconductor saturable absorber in transmission; SESAM: semiconductor saturable absorber mirror; BP: black phosphorous; FSF: frequency shifted feedback.

11.4.1 Saturable Absorbers

Saturable absorbers are passive optical switches, which are one of the most widely used approaches for pulse generation. They comprise a nonlinear optical material that exhibits decreasing absorption for increasing incident intensity, thus preferentially transmitting high-intensity light. When inserted into a resonant cavity, this allows ultrashort coherent pulses to build up over many round trips, seeded by noise fluctuations. The mechanism can also be explained in the frequency domain, noting that the saturable absorber modulates the light each round trip, thus adding sidebands to the signal, which injection-lock the phase of cavity modes that exist with approximately equal spacing. (For a thorough treatment of mode-locking and saturable absorber fundamentals, readers are recommended to consider a classic laser text, such as Ref. [1].) The parameters of the absorber such as the modulation depth, recovery time, saturation fluence and non-saturable loss all determine the laser steady state properties, and it remains an open problem to identify optimum mid-IR saturable absorbers to achieve stable mode-locking (i.e. opposed to the wide variety of other pulsed regimes that can be achieved in this way, such as Q-switching as discussed in Chapter 10).

11.4.1.1 Semiconductor Saturable Absorbers

Saturable absorbers are commercially available with varied parameters in the near-IR and are widely deployed practically. These are typically based on semi-

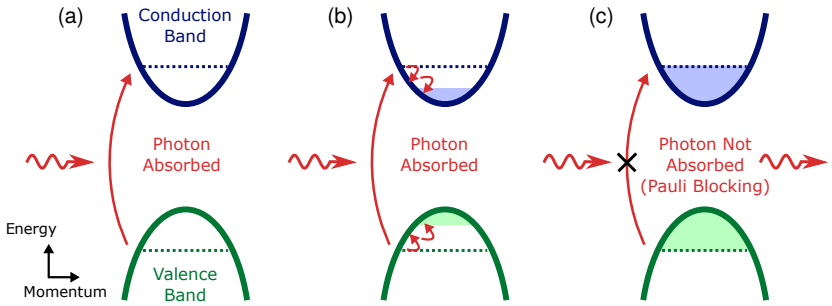

FIGURE 11.3 Illustration of semiconductor saturable absorption mechanism based on Pauli blocking. Simplified band structures are shown at three points of material excitation: (a) initially, incident photons are absorbed, exciting electrons from the valence band to the conduction band; (b) carriers in each band then rapidly thermalise, leaving unoccupied levels for further absorption and photoexcited electrons; (c) under intense illumination (on timescales shorter than material relaxation through carrier recombination), the upper states become fully occupied, forbidding further electrons being excited into the conduction band according to the Pauli exclusion principle and thus, saturating the absorption.

conductor quantum well layers on top of a mirror structure (forming a semiconductor saturable absorber mirror, SESAM) where the semiconductor is chosen for strong absorption at the laser wavelength (e.g. GaAs for 0.8 μm operation, InGaAs for 1 μm etc.). The physical mechanism for saturable absorption in semiconductors manifests from the excitation of electrons from the valence band to the conduction band under illumination (Fig. 11.3): for strong incident intensities, many electrons accumulate in the conduction band, filling the available upper states, thus the material is unable to absorb further photons according to the Pauli exclusion principle. After saturation, the material relaxes due to intraband thermalisation and electron-hole recombination, on a timescale governed by the 'relaxation time'.

At mid-IR wavelengths, the required narrow energy bandgap is naturally problematic for semiconductor technology. There have been a number of positive demonstrations using SESAMs (and semiconductor saturable absorbers in transmission, SESATs) in 3 μm fibre lasers, however. After the pioneering demonstration using thin InAs layers in 1996, researchers re-investigated indium-based SESAMs in mid-IR fibre lasers, starting in 2012 with Ho:ZBLAN fibre to achieve 24 ps pulses at 2.87 μm with 4.9 nJ energy [19], and later using Er:ZBLAN for 8.5 nJ pulses at 2.80 μm [13]. In the latter work, the authors showed that a minimum possible (i.e. Fourier transform-limited) pulse duration of 60 ps could be supported based on the measured 0.14 nm spectral bandwidth, although the pulse duration was not actually measured. We note that Table 11.1 only includes measured durations since it is well-known that numerous factors can lead to chirped pulses significantly broader than the transform limit, thus to fully characterise a mode-locked laser, a pulse measurement is essential (see Section 11.2).

Unfortunately, there has been limited work thoroughly characterising the nonlinear optical properties of mid-IR SESAMs. Many of the studies to date have employed a commercially available InAs device from BATOP [26], reported as offering 18% modulation depth, 10 ps relaxation time and 70 $\mu J/cm^2$ saturation fluence [14], but there are certainly opportunities for future work to investigate the optimisation of this specification and how it influences mode-locked laser performance. For example, a well-known criterion specifies that a laser's intracavity pulse energy E_p must exceed a certain threshold for stable continuous-wave mode-locking (i.e. avoiding Q-switching instabilities) [27]:

$$E_p^2 > E_{\text{sat,g}} E_{\text{sat,a}} \Delta R \tag{11.1}$$

where $E_{\text{sat,g}}$ is the saturation energy of the gain medium, $E_{\text{sat,a}}$ is the saturation energy of the absorber and ΔR is the modulation depth. The absorber saturation energy is related to its intrinsic saturation fluence $F_{\text{sat,a}}$ and incident beam area on the device A_a by: $E_{\text{sat,a}} = F_{\text{sat,a}} A_a$. While the saturation fluence of SESAMs cannot be changed in-situ, it is possible to vary the illuminated area on the device in a cavity using an imaging arrangement with lenses [19]. If the intracavity intensity is sufficient, a simpler approach is to butt-couple the saturable absorber directly to a fibre tip [11]. Alternatively, to achieve this criteria, the output coupling ratio can be carefully chosen (e.g. using custom-fabricated FBGs) to optimise the intracavity pulse energy to satisfy Eqn. 11.1 [13].

The recovery time of a saturable absorber is also critical, where a faster switching time typically permits shorter pulses (although it should be noted that careful laser designs exploiting soliton effects, for example, can lead to stable generation of pulses up to an order of magnitude shorter than the recovery time: known as the 'slow saturable absorber' operating regime [28]). The relatively long 10 ps relaxation time of mid-IR SESAMs to date may therefore have contributed to a lack of reported femtosecond SESAM-based lasers at 3 μm.

Furthermore, the prospects of indium-based saturable absorbers are limited for mid-IR pulse generation, as wavelengths beyond 3 μm approach the material's band edge. Therefore, other less well established semiconductor materials would need to be explored for mode-locking longer wavelengths (e.g. antimony layers could theoretically enable absorption up to 5 μm), but this has yet to be demonstrated in practice. Intense research effort has been directed towards the exploration of other types of saturable absorber materials, however, in the pursuit of broader operating bandwidths and improved performance.

11.4.1.2 Fe^{2+}:ZnSe Crystal Saturable Absorbers

An interesting suggestion was the use of an Fe^{2+}:ZnSe crystal as a saturable absorber. As noted in the introduction, Fe^{2+}:ZnSe can be used as a mid-IR gain medium, pumped between 2.5 and 3.5 μm for longer wavelength emission. By the nature of being a laser gain medium, the crystal can offer saturable absorption around 3 μm. This builds upon other studies in the near-IR showing

gain media to be useful saturable absorbers in the region where they strongly absorb [29]. Mode-locking using Fe^{2+}:ZnSe was demonstrated in Ref. [12] with an Er:ZBLAN laser at 2.78 μm. A stable 50 MHz pulse train was reported, with 0.93 nJ pulse energy, although an autocorrelation or FROG trace was not measured to quantify the duration.

Using Fe^{2+}:ZnSe as a saturable absorber has the advantage of offering excellent opto-mechanical characteristics, such as a high damage threshold, in addition to large saturable absorption cross section. However, the prospects for full-fibre integration of these components are poor since a bulk crystal is required. Additionally, the room-temperature upper state lifetime is 380 ns [5], which limits achievable pulse durations since this is longer than typical cavity transit times.

11.4.1.3 Nanomaterial Saturable Absorbers

The emerging class of low-dimensional nanomaterials, such as graphene, are currently experiencing broad research interest for many optical and electronic applications, not least as saturable absorbers due to their promising nonlinear optical characteristics [30, 31]. This interest arises for a variety of reasons. Firstly, such materials offer otherwise unachievable properties, e.g. relaxation times on femtosecond timescales and operation bandwidths exceeding those of classical semiconductors, in addition to the ability to 'tune' nanomaterial properties by varying the sample sizes (i.e. taking advantage of quantum mechanical size effects). Additionally, 2D materials are highly flexible in terms of their integration with optical components: they can be directly deposited onto mirrors or glass substrates (e.g. by spray coating or even inkjet printing) or incorporated with side-polished fibres and in polymer composites. While in the near-IR, polymer composites have shown greatest flexibility for integration of nanomaterials into fibre lasers, the existence of strong absorption for many polymers in the mid-IR, related to C-H bond resonances, has led to alternative integration strategies being preferred.

11.4.1.3.1 Graphene

Graphene was the first nanomaterial to be demonstrated for mid-IR pulse generation, being fabricated as a 4–6 layer film via chemical vapour deposition, which was then transferred onto a gold mirror [16]. The measured modulation depth of 10% and 2 MW/cm^2 saturation intensity resulted in the generation of stable 42 ps pulses with 0.7 nJ energy in a 2.8 μm Er:ZBLAN laser when one fibre facet was butted against the graphene-enhanced mirror, as shown in Fig. 11.4.

Graphene-coated metal mirrors are actually broadband ultrafast saturable absorbers, suitable for a range of laser wavelengths, arising from graphene's frequency-independent absorption of 2.3% per layer and sub-100-fs relaxation time [32]. However, nonlinear studies of few-layer graphene have revealed decreasing modulation depth at longer wavelengths: for example, Ref. [33]

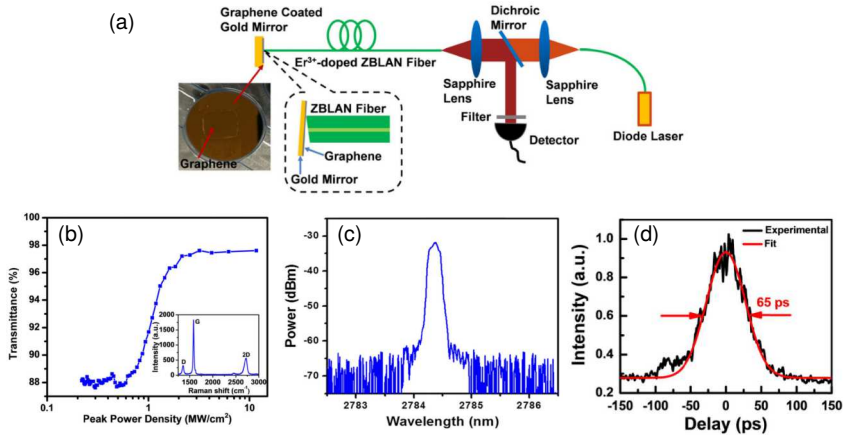

FIGURE 11.4 First graphene mid-IR mode-locked laser (after Ref. [16]): (a) cavity layout; (b) saturable absorber nonlinear transmission; (c) mode-locked spectrum; (d) autocorrelation trace.

observed that the maximum absorption modulation at 3 μm is less than half that at 1.5 μm. A corresponding increase in two-photon absorption (which acts against saturable absorption) was observed at longer wavelengths too. This could have a negative impact on mode-locking performance, since it is known from the Haus master equation that a greater modulation depth permits a larger stable mode-locking region of cavity parameter space [34]. However, we note that the discussed study [33] considered only tri-layer graphene and the authors comment that further investigation is required before generalizing their conclusions to all graphene devices. Additionally, damage to graphene saturable absorbers has been shown to be a limiting factor to power-scaling graphene-mode-locked lasers, highlighting additional opportunities for further work here to better understand and mitigate laser-induced damage.

11.4.1.3.2 Beyond Graphene

While graphene exhibits near-frequency-independent absorption, more recent research has focused on alternative 2D materials which are better suited to the mid-IR, in particular, black phosphorous. Black phosphorous is of particular interest for mid-IR nonlinear photonics as it is a layered material that possesses a thickness-dependent direct bandgap, varying from 0.3 eV (~4.1 μm) in bulk form (i.e. many layers) to 2 eV (0.62 μm) as a mono-layer, in addition to exhibiting ultrafast relaxation dynamics [35, 36].

A number of works have reported mid-IR pulse generation using black phosphorous [15, 21, 18]. At 2.8 μm, multilayer black phosphorous has been integrated in both erbium and holmium fibre lases for picosecond pulse generation by deposition onto gold mirrors. Pulse trains with 25.5 nJ, 42 ps pulses [15] (Fig. 11.5) and 6.3 nJ, 8.6 ps pulses [21] were produced, respectively (in both

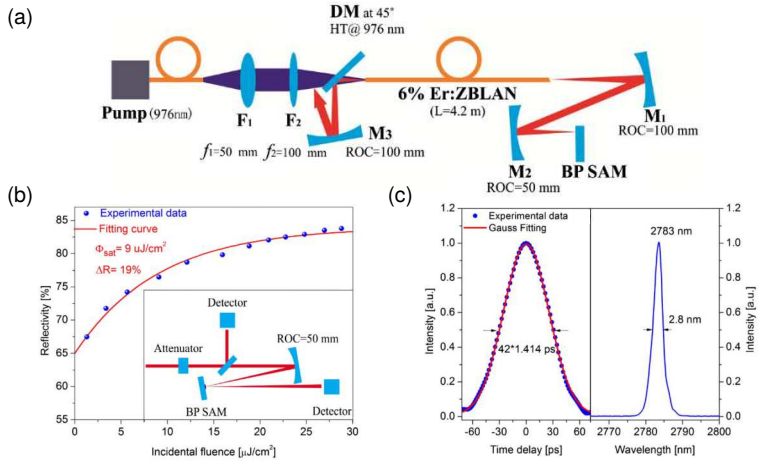

FIGURE 11.5 Black phosphorous mid-IR mode-locked laser (after Ref. [15]): (a) cavity layout; (b) saturable absorber nonlinear transmission; (c) autocorrelation trace & optical spectrum.

cases, the peak power was ~0.6 kW). It is also noteworthy that black phosphorous was used to mode-lock an Er:ZBLAN laser at 3.5 μm for the first time [18]. However, despite observing a stable 28.9 MHz pulse train, the authors of this study were unable to record an autocorrelation trace, preventing measurement of the pulse duration. It was shown, however, that the black phosphorous saturable absorber modulation depth of 19% at 2.8 μm was reduced to 7.7% at 3.5 μm [15, 18].

Finally, we note that researchers have also used Dirac semi-metal Cd_3As_2 for 10-ps pulse generation at 2.8 μm [23]. While less mature than black phosphorous, this nanomaterial family has the interesting feature of tunable relaxation time and saturation properties by adding additional dopants, indicating future prospects for carefully tailoring the saturable absorber properties.

Despite many fundamental studies showcasing remarkable properties of 2D materials, they have not yet demonstrated any significant tangible advantage over InAs SESAMs in 3 μm mid-IR fibre laser technology to date. While in the near-IR, femtosecond pulses have been routinely generated using nanomaterial saturable absorbers, in the mid-IR, the shortest pulse is 6.3 ps, similar to the results from SESAM mode-locking. Thus, the shorter relaxation timescales that have been reported for such nanomaterials have not been advantageous here. Further work is required to consider how to further reduce pulse durations of saturable absorber based mid IR lasers, in addition to critically comparing the differently families of absorber materials. However, the achievement of 3.5 μm mode-locking using black phosphorous (above the band edge of InAs) does highlight the wideband operation advantages over SESAMs for long-wavelength mode-locking, and novel all-fibre integration is also a promising avenue for

further work, e.g. deposition on side-polished fibres to take advantage of the nanomaterial platform.

11.4.2 Cavity Designs

Various mid-IR mode-locked fibre laser performance landmarks have also been achieved through novel cavity designs. For example, the impressive achievement of watt-level average power with 25 ps pulses at 2.78 μm from a SESAM-based Er:ZBLAN laser [14]. In this case, precautions such heat-sinking fibre tips in aluminium V-grooves to ensure efficient heat removal were required to avoid fibre damage. It is also well-known that parasitic reflections within a resonator can inhibit self starting of mode-locking, which is particularly problematic for high-power systems that include free-space sections around the fibre, with multiple exposed surfaces (each yielding 4% Fresnel reflection). To minimise this problem, the authors angle-cleaved the fibre and used reflective concave mirrors to focus onto the saturable absorber (rather than lenses). Their system produced 47 nJ energy pulses with 1.86 kW peak power, where the pulse peak power is computed as: $P_{\mathrm{pk}} = sE/\tau$ for energy E, full-width-at-half-maximum duration τ and shape factor s ($s = 0.94$ for Gaussian pulses, 0.88 for sech^2 pulse shapes). We note that the shape factor is occasionally erroneously omitted in the literature when calculating peak power; thus, we have ensured this is applied for the values presented in Table 11.1 for fair comparison.

With improvements to the cavity design, it has also been possible to reduce the pulse duration to ~6 ps [20, 17]. For example, Ref. [20] demonstrated a ring cavity [Fig. 11.6(c)–(d)], in contrast to linear cavities which are more typically employed due to simpler alignment and not requiring an isolator (which are currently only available in bulk form for the mid-IR). While linear cavities are able to produce stable ultrashort pulses, parasitic back reflections that destabilise mode-locking can be problematic, and thus, ring cavities can be advantageous. Apart from the exact emission wavelength, the choice between Er and Ho fibre has had minimal impact on picosecond mid-IR mode-locked fibre lasers to date; however, for femtosecond systems with broader pulse bandwidths, this can be an important factor, as discussed in Section 11.5.3.

Wavelength-tunable pulse trains have also been reported through the inclusion of a rotation diffraction grating into the cavity to provide a spectral filtering effect. Over 34 nm tunability (2.842–2.876 μm) was demonstrated from a Ho:ZBLAN SESAM-mode-locked laser producing 22 ps pulses [22] [Fig. 11.6(a)–(b)] and 90-nm tunability (2.71–2.82 μm) was shown from an Er:ZBLAN fibre pulse source with 6.4 ps pulse duration [17]. The record for tunability, however, is held by a dysprosium-doped fibre laser, using an electronically tunable acousto-optic tunable filter (AOTF) in the cavity to generate 33 ps pulses with over 330-nm tunability (2.97–3.3 μm) [25]. In this laser design, the AOTF also played an important role in the pulse generation process through frequency shifted feedback, which is an alternative pulse generation approach to

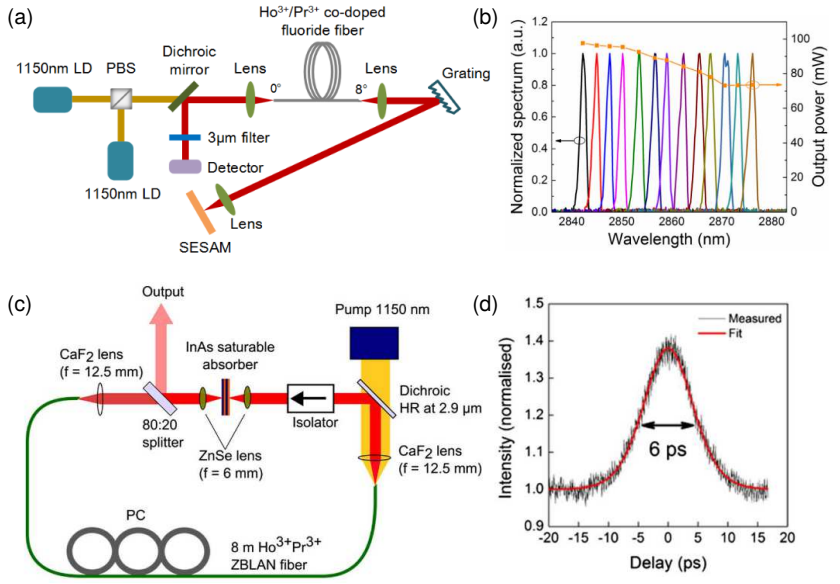

FIGURE 11.6 Novel mid-IR mode-locked cavity configurations. Wavelength-tunable mid-IR pulse generation using an intracavity diffraction grating (after Ref. [22]): (a) cavity layout; (b) tunable mode-locked spectra. Shortest pulses produced to date using a ring resonator with a semiconductor saturable absorber in transmission (after Ref. [20]): (c) cavity layout; (d) pulse autocorrelation trace.

saturable absorbers.

11.4.3 Frequency Shifted Feedback Mode-Locking

It is interesting to note that in the 1996 paper reporting the first mode-locked Er:ZBLAN fibre laser, in addition to InAs saturable absorber mode-locking, the authors also described a 'flying mirror mode-locking' experiment [11]. Here, an external cavity mirror was mounted on a loud-speaker driven with a periodic waveform, causing repetitive movement back-and-forth [Fig. 11.7(a)]. This mirror translation induced a Doppler frequency shift of light fed back into the cavity, which created new frequency components that were then amplified by the gain medium. During each movement cycle, pulse trains were observed at the laser output with pulse-to-pulse spacing corresponding to the cavity round-trip time—this certainly wasn't stable mode-locking and the authors were unable to measure the pulse profile or spectrum, however, it did highlight the potential to use intracavity frequency shifts for mid-IR pulse generation.

More recently, the concept of *frequency shifted feedback* (FSF) has been further studied and carefully harnessed in a Dy:ZBLAN laser [Fig. 11.7(b)] to achieve stable continuous picosecond pulse generation in the mid-IR [25]. The key cavity component to this mechanism was an intracavity AOTF (5 nm

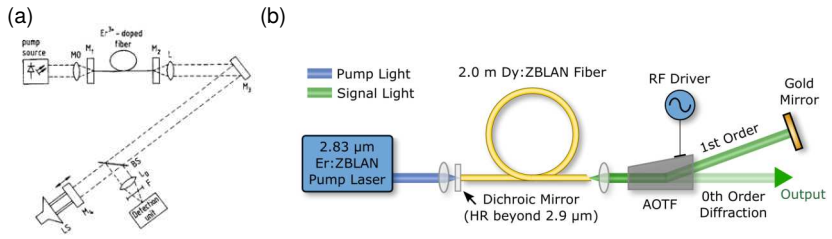

FIGURE 11.7 Pulse generation without a saturable absorber: (a) flying mirror mode-locking cavity (after Ref. [11]); (b) frequency shifted feedback mode-locking layout (after Ref. [25]).

bandwidth), comprising a TeO_2 crystal attached with an acoustic transducer and driven by a sinusoidal voltage. The driving voltage creates acoustic waves that propagate across the crystal. When light is incident on the device, only a narrow band of optical wavelengths meet the phase-matching condition for constructive interference with the acoustic waves, and this light is diffracted at a different angle to the undiffracted light which passes straight through. In addition to acting as a filter (where the central wavelength is determined by the acoustic wavelength, tunable by changing the frequency of the applied RF signal), the diffracted light is Doppler shifted by the travelling acoustic waves. By resonating this diffracted light, and taking the small portion of undiffracted light as output, a FSF laser cavity is formed [25].

FSF disrupts the longitudinal mode structure of the laser by continually shifting the frequency of light each round trip, eventually pushing it outside the gain bandwidth. However, the inclusion of nonlinearity in the cavity (e.g. Kerr nonlinearity from fibre) can cause intense light to spectrally broaden by self-phase modulation (SPM), which acts against the frequency shifting, enabling the signal to remain within the gain band. This is an intensity-discriminating effect, therefore favouring operation in a high-intensity short-pulse steady state. As SPM-generated light is phase coherent, the resulting steady state comprises a broader coherent spectrum, supporting picosecond pulses in the time domain [37]. We highlight that while this dynamic cannot rigorously be described as 'mode-locking' (since FSF inhibits longitudinal mode structure), the laser exhibits many characteristics that resemble typical mode-locking and in keeping with the existing literature, we adopt this term to describe this operating state. Note also that this is a 'passive' rather than 'active' pulse generation technique–the AOTF is driven with a constant RF sinusoid (it is not pulsed) and the pulse generation arises from nonlinear dynamics on the timescale set by the cavity length—the pulse repetition rate is thus equal to the inverse cavity round-trip time.

This FSF mode-locking approach was thoroughly investigated for early near-IR fibre lasers [37], but rarely used practically due to the widespread availability of SESAMs in the near-IR. In the mid-IR, however, as the identification of optimal

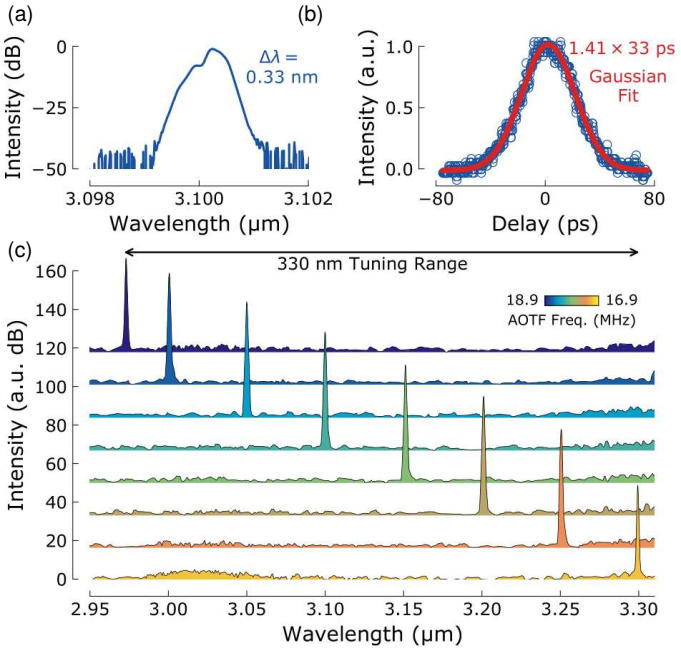

FIGURE 11.8 Dy:ZBLAN FSF laser output properties (after Ref. [25]): (a) optical spectrum; (b) autocorrelation trace; (c) wavelength-tunable spectra with varying AOTF drive frequency.

saturable absorber materials is still an open question (as discussed earlier), this mechanism has therefore been worthy of re-investigation and extension.

With a Dy:ZBLAN fibre cavity, this FSF technique generated 2.7 nJ pulses, broadly tunable from 2.97 to 3.30 μm, and with 33 ps duration (Fig. 11.8) [25]. The optical spectrum when mode-locked (Fig. 11.8(a)) showed noticeable broadening and asymmetry compared to non-mode-locked operation when the pump power was reduced (these features were also captured by numerical modelling, further explaining the FSF dynamics [25]).

Following this demonstration, FSF has also been applied using Ho:ZBLAN gain fibre, but this time using an acousto-optic modulator (AOM) in place of the intracavity AOTF [24]. This works on the same principles but the phase matching criteria is designed to operate for broader bandwidths (i.e. not explicitly applying a filtering effect), and thus the laser was not tunable. However, this arrangement generated 10 nJ pulses with 4.7 ps duration at 2.86 μm—the shorter duration compared to the AOTF Dy laser was attributed to the wider filter bandwidth, which has been theoretically shown to enable shorter pulses in FSF lasers [38]. The resulting peak power of 1.87 kW represents a current record for picosecond mid-IR fibre laser technology, confirming that FSF laser designs are an interesting addition to the toolbox of mode-locked mid-IR fibre laser engineers. Additionally, as TeO_2-based AOTFs are already commercially

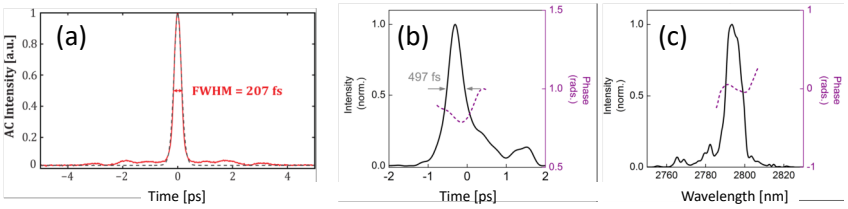

FIGURE 11.9 First measurements of sub-ps operation in erbium doped ZBLAN fibre lasers, operating at a central wavelength of 2.8 μm . (a) Autocorrelation of pulses from a 3 meter cavity with 3 kW peak power [39]. (b) Electric field envelope (retrieved via FROG) of a similar cavity arrangement. The uncompensated β_3 can be seen in the asymmetric pulse shape. This is likely observed in (a) as well, but appears as a symmetric side-lobe due to the autocorrelation. (c) Retrieved pulse spectrum with spectral phase plotted on the right axis.

available with operation from 2–4.5 μm, this could be a very useful technique for mid-IR pulse sources at even longer wavelengths.

11.5 STATE OF THE ART: FEMTOSECOND SYSTEMS

11.5.1 First Results

Sub-picosecond pulses in mid-IR fibre lasers were first achieved in 2015 (as shown in Fig. 11.9) [10, 39]. In both experiments, nonlinear polarisation evolution (NPE) was employed as an effective saturable absorber to achieve soliton mode-locking in an Er:ZBLAN fibre laser. Since these original demonstrations, the field has moved quickly to improve peak power [40, 41], employ other rare-earth ions to achieve femtosecond pulses at longer wavelengths [42], and use these pulses as drivers in nonlinear phenomenon [43, 44]. In this section, we review the state of the art in sub-ps mid-IR fibre lasers, discuss the favourable scaling of the soliton area theorem at long wavelengths, review advantages and disadvantages of various rare-earth ions for mode-locked mid-IR lasers, and briefly introduce nonlinear phenomenon driven by these systems.

The nonlinear polarisation evolution (NPE) mode-locking technique was first demonstrated by Hofer et al. in 1991 [45], building upon earlier demonstrations of intensity discrimination using birefringent silica fibres by Stolen, Botineau and Ashkin in 1982 [46]. In general, the index of refraction of a medium is given by $n = n_0 + n_2 I$, where n_0 is the linear index, n_2 is the nonlinear index and I is the instantaneous intensity of the propagating electric field. To understand the method by which NPE can be used to generate pulses, it useful to consider what happens to an optical pulse with elliptical polarisation. In this case, the high intensity of the central peak of the pulse will see a slightly different index of refraction relative to the lower intensity pulse wings (due to the $n_2 I$ term). Subsequently, the polarisation of the peak will rotate to a slightly different angle than the wings. In conjunction with a polarizing element, the lower intensity wings can be chopped off resulting in high loss for lower power

Ion	Wavelength μm	Bandwidth (nm)	Duration (fs)	Energy (nJ)	Peak Power (kW)	Year: Ref.
Er	2.8	20	497	3.6	6.4	2015: [47]
	2.8	25	207	0.8	3.5	2015: [39]
Ho/Pr	2.9	60	180	7.6	37	2016: [48]
Dy	3.1		828	4.8	4.2	2019:[42]

TABLE 11.2 State of the art in femtosecond mode-locked mid-infrared fibre lasers. Entries are left blank where the quantity was not measured / cannot be computed using the available data.

and low loss for high power (i.e. acting as an *artificial* saturable absorber). Since this phenomenon is dependent on the nonlinear index n_2, the response speed is determined by the electronic response of the material (typically <10 fs) and can thus be considered essentially instantaneous. Due to the simplicity of this method (only a few waveplates and a polariser are required) and the near instantaneous absorber recovery time, NPE in near-IR fibre lasers has become one of the most popular methods for obtaining ultrashort pulses.

11.5.2 Dispersion, Nonlinearity and Solitons in the Mid-IR

ZBLAN glass presents anomalous group velocity dispersion (GVD) throughout the mid-IR, from 1.7 μm to its transparency edge > 4 μm (Fig. 11.10(a)). Further, as most doped ZBLAN fibre has relatively large core sizes, waveguide dispersion can normally be ignored. This means that all demonstrations of rare-earth doped ZBLAN fibre lasers have been operated in a purely anomalous GVD regime (i.e. $\beta_2 < 0$), leading to soliton-based mode-locking. In this case, phase delays introduce by β_2 and SPM effects are balanced, leading to an ultrashort pulse that has a flat phase profile and a pulse energy given by the soliton area theorem:

$$E = \frac{2\beta_2}{\gamma A_{\text{eff}}} \tag{11.2}$$

where γ is the nonlinear parameter and A_{eff} is the effective area of the fibre mode. In the near-IR, the area theorem sets the limit on soliton pulse energy to values of typically 100's of pJ. This limitation was the driving factor behind many laser advances such as the dispersion-managed soliton laser and the all-normal dispersion (ANDi) laser which allows for pulse energies into the 10's of nJ. In the mid-IR, however, the soliton area theorem presents favourable scaling for creating higher pulse energy and peak power, before needing to consider dispersion management. The main difference is the nonlinear parameter γ, which is inversely proportional to both the wavelength and the effective area of the fibre. Since the core size of a *single-mode* fibre is directly proportional to wavelength, this means that the area of the fibre mode is proportional to

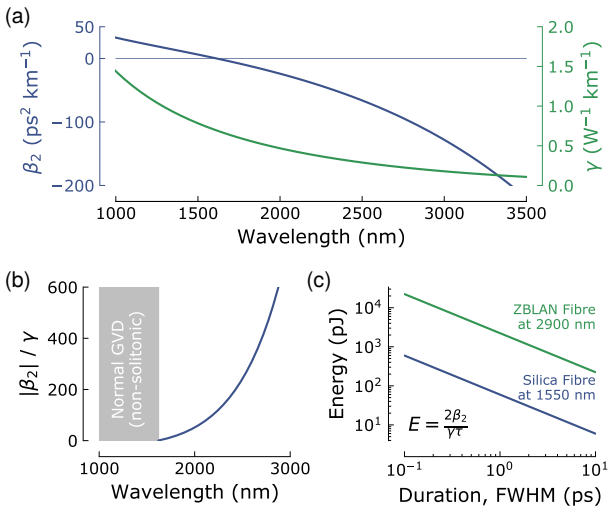

FIGURE 11.10 Properties of ZBLAN fibre (13 μm core diameter, 0.13 NA): (a) GVD & nonlinear parameter; (b) ratio of GVD to nonlinear parameter; (c) soliton energy–duration relationship at 2900 nm, compared to typical single-mode silica fibre (8.2 μm core diameter, 0.12 NA) at 1550 nm. Adapted from Ref. [49].

λ^2. Taken all together, this means the pulse energy in the soliton area theorem scales as λ^3, so simply by creating solitons at 2.9 μm instead of 1.5 μm, one can achieve >7× in pulse energy enhancement. Taking into account other differences in dispersion and nonlinearity between silica and ZBLAN glass that also scale favourably to ZBLAN, the typical mid-IR pulse energy enhancement is >10× relative to the near-IR (illustrated for a typical single-mode ZBLAN fibre in Fig. 11.10). Thus, while solitons in silica systems have been limited to sub-nJ levels, mid-IR Er and Ho ZBLAN systems have demonstrated > 7 nJ pulses with 10's of kW peak power. Through the favourable parameter scaling of the soliton area theorem, mid-IR ultrashort pulse fibre lasers can reach multi-10 kW peak powers directly from the cavity, without any need for recompression in free-space (e.g. as required if using dispersion management).

Multiple pulsing in soliton lasers, which is commonly observed in near-IR systems, occurs when the pump power is increased beyond a certain threshold. This threshold corresponds to the point at which the soliton pulse accrues excess energy and its nonlinear phase accumulation can no longer be compensated by the dispersive phase delay of the cavity. At this point, the soliton typically splits into two or more pulses which separate in time over many round trips in the laser cavity. This phenomenon was reported for mid-IR laser systems using a Ho/Pr mode-locked fibre laser [41], where fundamental soliton operation, three-pulse, and many pulse operation could all be achieved by simply adjusting the pump power.

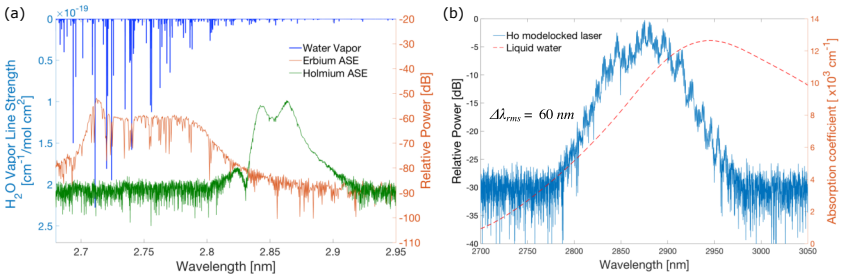

FIGURE 11.11 (a) Water vapour absorption lines overlaid with the ASE spectra of erbium- and holmium-doped ZBLAN. The strong absorption lines can be clearly seen on the erbium ASE spectrum. Beyond 2.8 μm however, the lines becomes much weaker. The holmium ASE spectrum, with a central emission around 2.9 μm, is much less affected by these water vapour lines. (b) Spectrum of Ho:ZBLAN mode-locked laser [41] showing minimal influence from water vapour absorption lines.

11.5.3 The Water-Vapour Problem

After the first reports of mode-locking in Er:ZBLAN, it became clear that water vapour absorption lines were playing a role in the mode-locked bandwidth of the laser [39, 10]. As shown in Fig. 11.11, the water vapour lines are quite strong throughout the gain bandwidth of the erbium ion. These absorption lines tend to limit the achievable mode-locked bandwidth, and thus pulse duration, through resonant-dispersive effects [40]. Reductions in the free-space section of the laser cavity or going to a truly all-fibre configuration (see Section 11.6.3 for an outlook on future devices) could help solve this problem, however free-space propagation in regular atmospheric conditions will still present significant attenuation of the pulse.

It was subsequently realised that moving to a gain medium with a slightly longer emission wavelength could help alleviate this problem. In 2016, Antipov et al. [41] achieved this by using the holmium ion, which emits near 2.9 μm, about 100 nm longer than erbium. This resulted in a significantly broader mode-locked bandwidth of nearly 60 nm (previous erbium lasers were approximately 20 nm). The pulse duration in this laser decreased to 180 fs, while the pulse energy rose to 7.6 nJ for a peak power of 37 kW directly from the oscillator. By comparison, using an Er:ZBLAN cavity with a similar free-space section, 3.6 nJ pulses with 6.4 kW peak power were achieved [10].

In 2019, Wang et al. [42] demonstrated a dysprosium ZBLAN laser operating at 3.1 μm. While the pulse width was relatively long (848 fs), dysprosium's wide bandwidth (~600 nm) makes this system a promising platform for the future. In principle, if the entire bandwidth of the dysprosium ion can be used for mode-locking, it would yield time-bandwidth limited pulse duration of < 30 fs—remarkably offering few-cycle pulses direct from the oscillator.

11.5.4 Technologies Driven by Ultrafast 3 μm Lasers

The 3 μm class mode locked fibre lasers present a great tool for driving nonlinear phenomena. With their high peak power and diffraction limited beam, the pulses from a 3 μm mode locked laser can be coupled with high efficiency into nonlinear fibres and amplifiers. One of the first experiments to take advantage of this used an Er:ZBLAN laser to drive soliton self-frequency shifting [43]. In this experiment, pulses from a mode-locked erbium system were coupled into a ZBLAN fibre with large overlap with the fundamental soliton. By varying the pulse energy, the amount of Raman based self-frequency shifting could be tuned to produce pulses between 2.8 and 3.4 μm.

One of the most studied nonlinear phenomena in optics is the generation of supercontinua via laser pulses. The last decade has seen an explosion of experiments aimed at creating supercontinua that cover the mid-IR and in particular the molecular fingerprint region (8-12 μm). Many of these experiments employ conventional OPA systems to generate mid-IR pump pulses to initiate the supercontinuum. These OPA systems are in turn built on high performance mode-locked near-IR lasers (quite often fibre lasers). Thus, an opportunity exists to simplify this scenario by driving the supercontinuum from an ultrashort pulse fibre laser operating fundamentally in the mid-IR.

The first such experiment using a 3 μm class mode locked fibre laser was reported in 2017 using a holmium system [44]. Over 4 kW peak power pulses were propagated through a chalcogenide microwire to generate light spanning from 2 to nearly 12 μm. As shown in Fig. 11.12, a chalcogenide rod was tapered down to a 3 μm core of As_2Se_3 to provide a γ of 2.92 $W^{-1}m^{-1}$ at the pulse's centre wavelength of 2.87 μm. At this dimension, the 5 cm long microwire provided fully normal dispersion and good confinement up to around 8 μm. As the supercontinuum broadened to beyond 8 μm, the optical mode in the microwire core expanded significantly into the As_2S_3 cladding, thus dropping the nonlinear parameter by more 20 times. Nevertheless, an average power spectral density of 0.003 mW/nm was achieved over a bandwidth of 2.4 octaves in the mid-IR. While improvements can certainly be made, systems such as this one are promising alternatives to current technology for high brightness mid-IR supercontinuum sources.

11.6 FUTURE DIRECTIONS

This Chapter has shown that mode-locked mid-IR fibre lasers have come a long way since their first demonstration in 1996, and landmark performance records continue to be reported each year. It is also noteworthy that ultrafast 3 μm fibre laser technology has recently been commercialised by Femtum [50], paving the road to real-world deployment and exploitation of recent research developments. Alongside such practical advances, there are also a number of promising future directions for the field to further improve mode-locked mid-IR systems, which

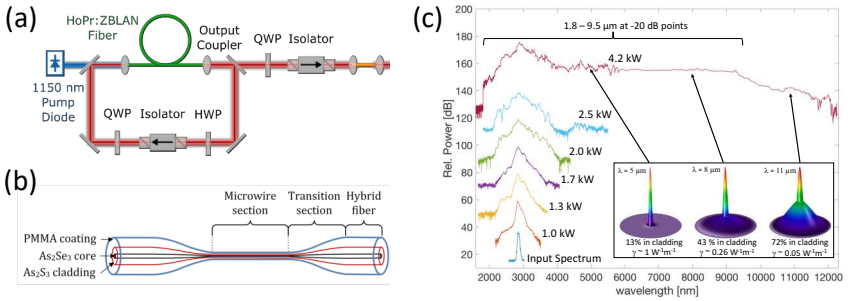

FIGURE 11.12 (a) Layout of the supercontinuum driven by a holmium mode-locked fibre laser. (b) Schematic of the chalcogenide microwire. The microwire section is 5 cm long with a tapered core diameter of 3 μm (cladding diameter = 28 μm). (c) Supercontinuum generated from the microwire as a function of coupled peak power. Inset shows the calculated (COMSOL) mode shape in the core at various wavelengths. Significant broadening into the microwire cladding leads to reduced nonlinearity at longer wavelengths. Adapted from Ref. [44].

we now briefly consider, concluding this Chapter with critical consideration of the opportunities that lie ahead.

11.6.1 Dispersion Engineering in the Mid-IR

As discussed in Section 11.5.2, dispersion and nonlinearity have a major influence on the mode-locked steady-state properties. It was shown how a balance between anomalous group-velocity dispersion and Kerr nonlinearity could produce soliton pulses, with energy defined by the fibre properties. While the stronger anomalous dispersion and weaker nonlinearity of ZBLAN fibre, compared to silica fibre in the near-IR, enables higher energy solitons, their energy is still ultimately limited by soliton quantisation. It is therefore instructive to consider how this limit may be circumvented through dispersion engineering in the mid-IR, building on sustained work in the near-IR which has has led to the discovery of many novel pulse shaping regimes through careful control of net cavity dispersion [49, 51].

Multi-pulsing of mode-locked soliton lasers is caused by excessive nonlinear phase accumulation. Therefore, one strategy to mitigate this is to implement a cavity ‘dispersion map’: including sections of normal and anomalous dispersion causing the pulse to periodically broaden and compress during a single round-trip, thus reducing the path-averaged peak power (known as a stretched-pulse laser [52]). To balance the strong anomalous dispersion of ZBLAN glass at 3 μm, chalcogenide fibres (such as As_2S_3 fibres that are already commercially available) could be included, which typically have zero dispersion wavelengths beyond 5 μm (i.e. are highly normally dispersive around 3 μm). While there are both material and waveguide contributions to the total fibre dispersion, the material dispersion component (Fig. 11.10) is dominant for typical step-index

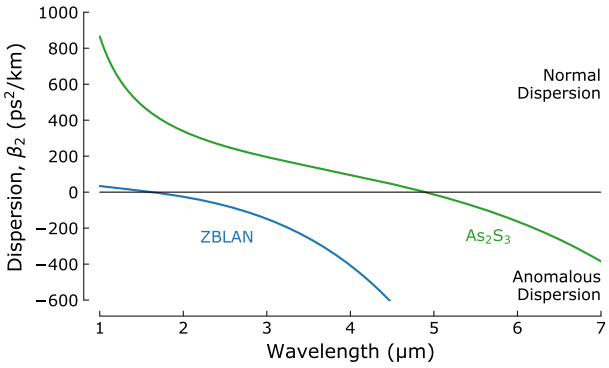

FIGURE 11.13 Material group velocity dispersion curve for ZBLAN and chalcogenide As_2S_3.

mid-IR fibre geometries.

An additional advancement would be to employ an all-normal-dispersion (ANDi) laser design, building on work in the near-IR which showed the avoidance of soliton limitations by removing anomalous dispersion from the cavity [53]. At present, however, all mid-IR fibre lasers have employed anomalously dispersive fluoride glasses. Similar enhancements to maximum possible pulse energies could still be achieved though, by including sufficient chalcogenide fibre to give large net-normal cavity dispersion, or a custom-made chirped FBG for lumped dispersion compensation. Furthermore, recent progress in the fabrication of rare-earth-doped chalcogenide glasses raises the prospects for simpler implementations in the future by simply removing anomalously dispersive fibre. Recent theoretical analysis has suggested that impressive >100 nJ pulse energies could be achieved from such a net-normal dispersion Er:ZBLAN laser, compressible to ~100 fs [54], highlighting that this is certainly a promising future avenue to explore .

11.6.2 Mode-Locking at Longer Wavelengths: Towards 4 μm Ultrafast Fibre Lasers

All mode-locked mid-IR fibre lasers to date have generated pulses in the 2.7–3.5 μm region. There have been demonstrations of ultrafast fibre-based pulse generation at longer wavelengths, but these have all required the exploitation of nonlinear optical phenomena such as soliton self-frequency shift, pumped by shorter wavelength lasers [55]. Despite these impressive results, there is still demand for fibre pulse sources emitting beyond 4 μm, for example to target certain absorption resonances or for applications requiring free-space propagation, within the 3–5 μm atmospheric transmission window.

To meet this need, 4 μm-class fibre lasers are currently surfacing, using

lower phonon energy indium fluoride InF_3-based glasses in place of ZBLAN. CW lasing at 3.9 μm from the $^5I_5 \rightarrow ^5 I_6$ transition in Ho:InF_3 has been reported [56], in addition to initial observation of fluorescence emission from 4.1 to 4.5 μm in Dy:InF_3 [57]. While there remains much work to better understand their spectroscopy and optimisation of CW lasing first, it is expected that application of the mode-locking techniques described in this chapter could be applied for short-pulse generation in these systems. As InF_3 has a similar dispersion profile to ZBLAN, even with these existing designs the favourable soliton energy scaling relationship (Section 11.5.2) suggests that fluoride fibre-based 4 μm mode-locked lasers could achieve 10s nJ pulse energies without requiring dispersion management.

11.6.3 All-Fibre Configurations with Emerging Components

One of the main challenges facing current mid-IR ultrashort pulse fibre lasers is their requirement of free-space sections within the laser cavity. This is due to the lack of all-fibre components such as wavelength-division multiplexers, splitter/couplers, and integrated isolators. Two significant problems arise from this situation. The first is that the stability and robustness of the laser system is dramatically reduced relative to truly all-fibre laser systems since free-space alignment must be maintained. The second problem is that OH- ingress into ZBLAN fibre occurs when a ZBLAN fibre tip is exposed to the atmosphere. In certain situations [58], simply doubling the laser pump power can decrease the tip lifetime by > 6 times. While fusion-splicing multimode AlF_3 end-caps onto the ZBLAN fibre tip can help alleviate this problem, at higher power operation even this method fails [59]. Thus, for mid-IR fibre lasers to achieve widespread use and make contributions to industrial applications, all-fibre components must be developed.

Current attempts at creating all-fibre components that operate beyond 2 μm however, have had limited success. By adapting techniques from fused fibre technology in silica glass, Stevens and Woodbridge [60] demonstrated low ratio ZBLAN couplers (i.e. 1-10% coupling) with total insertion loss of < 1 dB. However, for higher coupling ratios (i.e. ~50%) the insertion loss increased to 2-3 dB due to localised necking and surface defects in the ZBLAN glass. Improving this performance will require improved control over the initial fabrication of the ZBLAN fibre as well as tighter tolerances on the tapering process. Using chalcogenide glass offers yet another platform for components.

Chalcogenide glass fibres, including As_2S_3/Se_3, have been tapered for non-linear applications in the near-IR since 2007 [61, 62, 63]. In the mid-IR, fused fibre power combiners are now commercially available from IRFlex [64]. However, key fibre laser components such as wavelength-division multiplexers and single-mode splitters remain firmly in the research realm.

An alternative approach to fused fibre technology is hybrid bulk-fibre devices. In this platform, a hybridised device is created consisting of ZBLAN or

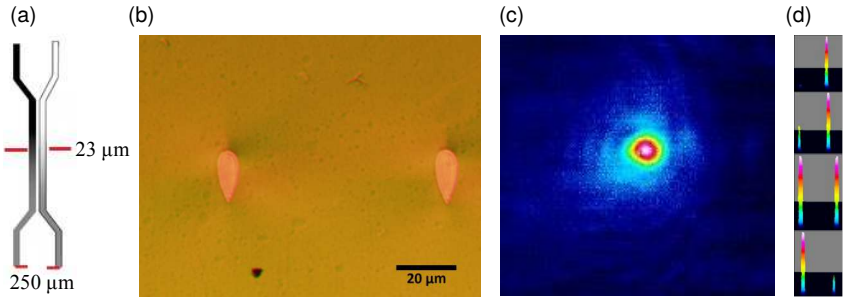

FIGURE 11.14 (a) Schematic of direct-write waveguide coupler in GLS. (b) End-facet view of GLS waveguides spaced at 250 µm. (c) Mode image of 3 µm light at the output of GLS waveguide. (d) Power splitting measurements of a 2 waveguide coupler for a range of coupling coefficients.

chalcogenide fibre connected to direct-write waveguides in bulk mid-IR glasses. Femtosecond laser micro-machining direct-write techniques [65] can yield low-loss waveguides in various mid-IR glasses including ZBLAN and GLS (see Fig. 11.14). As these waveguides are created by translating the glass through a beam of femtosecond pulses, complex waveguide shapes can be created allowing for splitters and WDMs. In 2014, Arriola et al. [66] demonstrated directional couplers in gallium lanthanum sulfide (GLS) glass with propagation losses of < 0.8 dB/cm and splitting ratios between 8 % and 99% at a wavelength of 3.39 µm. GLS is particularly interesting as the directly written waveguides have numerical apertures and mode areas commensurate with standard ZBLAN optical fibre. Commercial pig-tailing stations that are commonplace in silica component manufacturing can in principle be used to turn these GLS chips into fully functional, low-loss mid-IR components.

It is also worth mentioning that some components do not need multiple waveguides to achieve their functionality. Such is the case for an in-line polariser. Using direct-write techniques, Bharathan et al. created 45° tilted FBGs in a ZBLAN single-mode fibre which resulted in an all-fibre polariser capable of producing ~ 20 dB polarisation extinction ratio in a laser cavity [67]. This device could find practical application in the NPE mode-locked systems described in the preceding sections of this chapter, removing the need for bulk polarisers.

11.6.4 Chirped Pulse Amplifiers

The advent of ultrafast mid-IR fibre lasers has paved the way for chirped-pulse amplification (CPA) [68]. In this technique, the ultrashort pulse is first chirped to the many picosecond level to reduce the peak power, then the pulse energy is greatly increased in an amplifier before being recompressed using free-space dispersive components (e.g. gratings). This procedure allows for the creation of high energy pulses with extraordinary peak power far beyond the damage threshold of the amplifying medium. In the near-IR, CPA systems have transformed applications such as laser eye surgery and micro-machining for medical devices.

Indeed, the importance of this technique was recognised by the 2018 Nobel Prize in Physics.

Although CPA systems have yet to be demonstrated with mid-IR fibre lasers, the necessary pieces (i.e. the amplifier [43] and the compressor [69]) have each individually been established. With the amplifier in Ref. [43], up to 37 nJ pulses were achieved, while with the compressor of Ref. [69], pulses could be recompressed to 70 fs (only 15 % longer than the time-bandwidth limit). Looking ahead, it is conceivable that pulse energies approaching 100 nJ with durations of 150 fs (limited by the Erbium transition's gain bandwidth) could be created in these systems provided mechanisms such as end-caps are in place to limit damage to the ZBLAN fibre. The increased pulse peak power could then drive further spectral broadening in a nonlinear compressor setup, enabling compression to single-cycle durations (~10 fs at 3 μm).

11.6.5 Dual-Comb Spectroscopy with Mid-IR Fibre Lasers

Dual-comb spectroscopy (DCS) has emerged in recent years as one of the most powerful tools in spectroscopic measurement [70]. In this scheme, two mode-locked laser pulse trains with slightly different repetition frequencies are overlapped on a photodetector to produce a heterodyne RF comb spectrum. If one or both of the pulse trains interacts with a molecule and experiences absorption loss at a particular wavelength, then that information is translated to the RF domain via the heterodyne beat. In this way, the entire optical absorption spectrum of the pulse trains can be mapped to the RF domain and analysed. This technique allows for broad wavelength measurement on the μs to ms timescale with high resolution (i.e. 1 kHz to 1 MHz).

The vast majority of these systems, however, have been demonstrated in the near-IR with silica based fibre lasers. This is an unfortunate situation since the strongest molecular absorption lines exist in the mid-IR beyond 2 μm. Using a 3 μm ultrashort pulse fibre laser this situation could change significantly. As demonstrated in Ref [44], 3 μm fibre lasers can already drive supercontinuum to 12 μm. Thus, with an appropriate second mode-locked laser, a mid-IR fibre laser driven DCS system could span all of the functional region (2–6.7 μm) and much of molecular fingerprint region (6.7–20 μm) of the mid-IR.

Based on the current performance of mode-locked mid-IR fibre lasers presented in this chapter, up to 3 μm W/nm should be achievable from ~6 μm to 12 μm. Relative to the conventional globar systems found in modern FTIRs, this corresponds to a brightness increase of > 10^6. Furthermore, the diffraction-limited output would allow for collimation and transfer over long distances to perform spectroscopic measurement over km-scale distances.

11.7 CONCLUSION

Although rare-earth doped ZBLAN fibre lasers are now more than 30 years old, ultrafast operation in these systems was demonstrated only in the current decade [10, 39]. While we can only speculate on the origin of the delay between demonstrations of CW versus sub-picosecond mode-locked operation, one thing is clear: mid-IR ultrafast fibre lasers are now rapidly developing and their performance is beginning to challenge traditional laser systems. Indeed, the nearly 40 kW peak power pulses from the holmium doped ZBLAN system described in Section 11.5 already out-performs many commercial OPA systems operating near 3 μm. Furthermore, with nonlinear techniques such as soliton self-frequency shifting [43] mid-IR ultrafast pulses can access a wavelength range spanning 2.8 to 3.6 μm. In combination with chalcogenide microwires, supercontinuum can be generated spanning from 2 to 12 μm. Finally, with an intra-cavity AOTF (Section 11.4.3), FSF mode-locking can be achieved and rapid wavelength-sweeping of picosecond pulses could be created and used for sensing applications [71]. All of these demonstrations add to the growing sentiment that ultrafast mid-IR fibre lasers will be a disruptive technology in the coming years.

However, several hurdles remain for these laser systems. The most significant barrier is the lack of all-fibre ZBLAN components. The field of ultrafast near-IR fibre lasers has enjoyed the benefits of the robust materials properties of silica glass and abundance of cheap, high performance components. This situation was made possible by the massive investment made by the telecommunications industry over several decades, leading to ultra low-loss fibre, high gain amplifiers, cheap pump diodes, a wide array of all-fibre components and a long list of high performance characterisation tools (fast photodiodes, spectrometers, FROGs, etc.). As ZBLAN optical fibre did not see this same level of investment and research, it lags behind silica in every respect. Things are improving, though, with the first all-fibre couplers recently appearing on the market and the list ZBLAN suppliers consistently growing. To achieve broad appeal for scientists in fields other than laser science, however, the situation needs to be similar to what is found in the near-IR. If the components required to use these systems in general experiments are developed to the necessary level soon, we may see disruption in a range of fields.

It is early to speculate on which fields and applications will be most significantly impacted, but we can draw some conclusions by examining the current state of applications using conventional systems. Spectroscopy in both the functional and fingerprint regions of the mid-IR has long been pursued due to the sensitivity and specificity one can achieve using these wavelengths. At the moment, most mid-IR spectral measurements are achieved with commercial FTIR systems which in turn rely on low brightness blackbody filaments. The limited brightness of these *globars* means that both sensitivity and measurement speed are limited. This picture could change with an all-fibre mid-IR spanning supercontinuum similar to that presented in section 11.5.4. A fibre laser based

supercontinuum source would be on the order of 1000 times brighter than the traditional globars and the collimated beam could allow for stand-off measurements on the order of kilometres.

Materials processing could also see significant improvement with ultrashort pulse mid-IR fibre laser systems. Of particular interest in this application are human tissue surgery and plastic processing. As human tissues tend to have high water content, ultrashort pulse systems operating near the water absorption peak at 2.95 μm offer the possibility for improved surgical incision. In this application, the high intensity fibre laser pulses are strongly absorbed in the superficial layer of the tissue leading to precise shaping through tissue ablation. Using pulses from a conventional free-space laser, the efficacy of this technique has been demonstrated with reduced scarring and faster recovery time [72]. Moving to a mode-locked fibre laser system based on either erbium or holmium would allow for robust power scaling and flexible delivery, both of which are significant advantages in a surgical environment. Similarly, shaping and cutting plastics is of ever-increasing importance in technology and society in general. Using the strong absorption of hydrocarbon-based polymers at 3.2 μm, precision processing can be achieved. Emerging dysprosium mode-locked systems and long-wavelength erbium systems could one day offer compact, high performance solutions for this application.

The coming decade will likely see several important advances in the state-of-the-art including: new materials for robust saturable absorber mode-locking in the mid-IR, low-loss all-fibre components based on ZBLAN and other soft-glass platforms, and significant improvements in ultrafast performance with a strong potential for mid-IR fibre laser based frequency combs.

Bibliography

[1] Anthony E Siegman. *Lasers*. University Science Books, 1986.

[2] Irina T Sorokina and Konstantin L Vodopyanov. *Solid-state mid-infrared laser sources*. 2003.

[3] Majid Ebrahim-Zadeh and Irina T. Sorokina. *Mid-Infrared Coherent Sources and Applications*. Springer, 2008.

[4] U. Elu, M. Baudisch, H. Pires, F. Tani, M. H. Frosz, F. Kottig, A. Ermolov, P. St. J. Russell, and J. Biegert. High average power and single-cycle pulses from a mid-IR optical parametric chirped pulse amplifier. *Optica*, 4(9):1024, 2017.

[5] Sergey B. Mirov, Vladimir V. Fedorov, Dmitry Martyshkin, Igor S. Moskalev, Mike Mirov, and Sergey Vasilyev. Progress in mid-IR lasers based on Cr and Fe-doped II-VI chalcogenides. *IEEE J. Sel. Top. Quantum Electron.*, 21(1):1601719, 2015.

[6] Chee Leong Tan and Hooman Mohseni. Emerging technologies for high performance infrared detectors. *Nanophotonics*, 7(1):169–197, 2018.

[7] Hamamatsu. *Characteristics and use of infrared detectors*. 2011.

[8] Rick Trebino. *Frequency-Resolved Optical Gating: The Measurement of Ultrashort Laser Pulses*. Springer, 2000.

[9] P. K. Bates, O. Chalus, and J. Biegert. Ultrashort pulse characterization in the mid-infrared. *Opt. Lett.*, 35(9):1377, 2010.

[10] Tomonori Hu, Stuart. D. Jackson, and Darren. D. Hudson. Ultrafast pulses from a mid-infrared fiber laser. *Opt. Lett.*, 40(18):4226, 2015.

[11] Christian Frerichs and Udo B. Unrau. Passive Q-switching and mode-locking of erbium-doped fluoride fiber lasers at 2.7 μm. *Opt. Fiber Technol.*, 2(4):358–366, 1996.

[12] Chen Wei, Xiushan Zhu, R A Norwood, and N Peyghambarian. Passively contiuous-wave mode-locked Er3+-doped ZBLAN fiber laser at 2.8 um. *Opctics Lett.*, 37(18):3849, 2012.

[13] Adil Haboucha, Vincent Fortin, Martin Bernier, Jérôme Genest, Younès Messaddeq, and Réal Vallée. Fiber Bragg grating stabilization of a passively mode-locked 2.8 μm Er3+: fluoride glass fiber laser. *Opt. Lett.*, 39(11):3294, 2014.

[14] P. Tang, Z. Qin, J. Liu, C. Zhao, G. Xie, S. Wen, and L. Qian. Watt-level passively mode-locked Er3+-doped ZBLAN fiber laser at 2.8 μm. *Opt. Lett.*, 40(21):4855–4858, 2015.

[15] Zhipeng Qin, Guoqiang Xie, Chujun Zhao, Shuangchun Wen, Peng Yuan, and Liejia Qian. Mid-infrared mode-locked pulse generation with multilayer black phosphorus as saturable absorber. *Opt. Lett.*, 41(1):56, 2016.

[16] Gongwen Zhu, Xiushan Zhu, Fengqiu Wang, Shuo Xu, Yao Li, X. Guo, K. Balakrishnan, R. A. Norwood, and N. Peyghambarian. Graphene mode-locked fiber laser at 2.8 μm. *IEEE Photon. Technol. Lett.*, 28(1):7, 2016.

[17] Yanlong Shen, Yishan Wang, Hongwei Chen, Kunpeng Luan, Mengmeng Tao, and Jinhai Si. Wavelength-tunable passively mode-locked mid-infrared Er3+-doped ZBLAN fiber laser. *Sci. Rep.*, 7:14913, 2017.

[18] Z. Qin, T. Hai, G. Xie, J. Ma, P. Yuan, L. Qian, L. Li, L. Zhao, and D. Shen. Black phosphorus Q-switched and mode-locked mid-infrared Er:ZBLAN fiber laser at 3.5 μm wavelength. *Opt. Express*, 26(7):8224, 2018.

[19] Jianfeng Li, Darren D. Hudson, Yong Liu, and Stuart D. Jackson. Efficient 2.87 μm fiber laser passively switched using a semiconductor saturable absorber mirror. *Opt. Lett.*, 37(18):3747, 2012.

[20] Tomonori Hu, Darren D. Hudson, and Stuart D. Jackson. Stable, self-starting, passively mode-locked fiber ring laser of the 3 μm class. *Opt. Lett.*, 39(7):2133–2136, 2014.

[21] J F Li, H Y Luo, B Zhai, R G Lu, Z N Guo, H Zhang, and Y Liu. Black phosphorus: a two-dimension saturable absorption material for mid-infrared Q-switched and mode-locked fiber lasers. *Sci. Rep.*, 6(April):11, 2016.

[22] Chen Wei, Hongxia Shi, Hongyu Luo, Han Zhang, Yanjia Lyu, and Yong Liu. 34 nm-wavelength-tunable picosecond Ho3+/Pr3+-codoped ZBLAN fiber laser. *Opt. Express*, 25(16):19170, 2017.

[23] Chunhui Zhu, Fengqiu Wang, Yafei Meng, Xiang Yuan, Faxian Xiu, Hongyu Luo, Yazhou Wang, Jianfeng Li, Xinjie Lv, Liang He, Yongbing Xu, Junfeng Liu, Chao Zhang, Yi Shi, Rong Zhang, and Shining Zhu. A robust and tuneable mid-infrared optical switch enabled by bulk Dirac fermions. *Nat. Commun.*, 8:14111, 2017.

[24] M. R. Majewski, R. I. Woodward, and S. D. Jackson. Ultrafast mid-infrared fiber laser mode-locked using frequency-shifted feedback. *Opt. Lett.*, 44(7):1698, 2019.

[25] R. I. Woodward, M. R. Majewski, and S. D. Jackson. Mode-locked dysprosium fiber laser: picosecond pulse generation from 2.97 to 3.30 μm. *APL Photonics*, 3(11):116106, 2018.

[26] BATOP Saturable Absorbers, https://www.batop.de/products/saturable-absorber/saturable-absorber.html.

[27] C Hönninger, R Paschotta, F Morier-Genoud, M. Moser, and U. Keller. Q-switching stability limits of continuous-wave passive mode locking. *J. Opt. Soc. Am. B*, 16(1):46–56, 1999.

[28] R. Paschotta and U. Keller. Passive mode locking with slow saturable absorbers. *Appl. Phys. B*, 73(7):653–662, nov 2001.

[29] Yen-Kuang Kuo, Milton Birnbaum, and Wei Chen. Ho:YLiF 4 saturable absorber Q -switch for the 2-μm Tm,Cr:Y3Al5O12 laser. *Appl. Phys. Lett.*, 65(24):3060–3062, 1994.

[30] R. I. Woodward and E. J. R. Kelleher. 2D saturable absorbers for fibre lasers [Invited]. *Appl. Sci.*, 5(4):1440–1456, 2015.

[31] Grzegorz Sobon. Mode-locking of fiber lasers using novel two-dimensional nanomaterials: graphene and topological insulators [Invited]. *Photon. Res.*, 3(2):A56, 2015.

[32] Zhipei Sun, Tawfique Hasan, Felice Torrisi, Daniel Popa, Giulia Privitera, Fengqiu Wang, Francesco Bonaccorso, Denis M Basko, and Andrea C Ferrari. Graphene mode-locked ultrafast laser. *ACS Nano*, 4(2):803–10, 2010.

[33] Andrew Malouf, Ori Henderson-Sapir, Sze Set, Shinji Yamashita, and David J. Ottaway. Two-photon absorption and saturable absorption of mid-IR in graphene. *Appl. Phys. Lett.*, 114(9):091111, 2019.

[34] Herman A. Haus. Mode-locking of lasers. *IEEE J. Sel. Top. Quantum Electron.*, 6(6):1173–1185, 2000.

[35] Xiaomu Wang and Shoufeng Lan. Optical properties of black phosphorus. *Adv. Opt. Photonics*, 8(4):618, 2016.

[36] Meng Zhang, Qing Wu, Feng Zhang, Lingling Chen, Xinxin Jin, Yuwei Hu, Zheng Zheng, and Han Zhang. 2D black phosphorus saturable absorbers for ultrafast photonics. *Adv. Opt. Mater.*, 7(1):1800224, 2019.

[37] Hendrik Sabert and Ernst Brinkmeyer. Pulse generation in fiber lasers with frequency shifted feedback. *J. Light. Technol.*, 12(8):1360–1368, 1994.

[38] C. Martijn de Sterke and M. J. Steel. Simple model for pulse formation in lasers with a frequency-shifting element and nonlinearity. *Opt. Commun.*, 117(5-6):469–474, 1995.

[39] Simon Duval, Martin Bernier, Vincent Fortin, Jérôme Genest, Michel Piché, and Réal Vallée. Femtosecond fiber lasers reach the mid-infrared. *Optica*, 2(7):623, 2015.

[40] Simon Duval, Michel Olivier, Vincent Fortin, Martin Bernier, Michel Piché, and Réal Vallée. 23-kW peak power femtosecond pulses from a mode-locked fiber ring laser at 2.8 μm. *Fiber Lasers XIII Technol. Syst. Appl.*, 9728:972802, 2016.

[41] Sergei Antipov, Darren D. Hudson, Alexander Fuerbach, and Stuart D. Jackson. High-power mid-infrared femtosecond fiber laser in the water vapor transmission window. *Optica*, 3(12):1373–1376, 2016.

[42] Yuchen Wang, Frédéric Jobin, Simon Duval, Vincent Fortin, Paolo Laporta, Martin Bernier, Gianluca Galzerano, and Réal Vallée. Ultrafast Dy3+:fluoride fiber laser beyond 3 μm. *Opt. Lett.*, 44(2):395, 2019.

[43] Simon Duval, Jean-Christophe Gauthier, Louis-Rafaël Robichaud, Pascal Paradis, Michel Olivier, Vincent Fortin, Martin Bernier, Michel Piché, and Réal Vallée. Watt-level fiber-based femtosecond laser source tunable from 2.8 to 3.6 μm. *Opt. Lett.*, 41(22):5294, 2016.

[44] D. D. Hudson, S. Antipov, L. Li, I. Alamgir, T. Hu, M. E. Amraoui, Y. Messaddeq, M. Rochette, S. D. Jackson, and A. Fuerbach. Toward all-fiber supercontinuum spanning the mid-infrared. *Optica*, 4(10):1163, 2017.

[45] M. Hofer, M. E. Fermann, F. Haberl, M. H. Ober, and A. J. Schmidt. Mode locking with cross-phase and self-phase modulation. *Opt. Lett.*, 16(7):502, 1991.

[46] R H Stolen, J Botineau, and A Ashkin. Intensity discrimination of optical pulses with birefringent fibers. *Opt. Lett.*, 7(10):512–514, 1982.

[47] Jonathan Hu, Curtis R. Menyuk, Chengli Wei, L. Brandon Shaw, Jasbinder S. Sanghera, and Ishwar D. Aggarwal. Highly efficient cascaded amplification using Pr3+-doped mid-infrared chalcogenide fiber amplifiers. *Opt. Lett.*, 40(16):3687, 2015.

[48] Sergei Antipov, Martin Ams, Robert J. Williams, Eric Magi, Michael J. Withford, and Alexander Fuerbach. Direct infrared femtosecond laser inscription of chirped fiber Bragg gratings. *Opt. Express*, 24(1):30, 2016.

[49] R. I. Woodward. Dispersion engineering of mode-locked fibre lasers [Invited]. *J. Opt.*, 20:033002, 2018.

[50] Femtum: https://www.femtum.com. 2019.

[51] William H Renninger, Andy Chong, and Frank W Wise. Pulse shaping and evolution in normal-dispersion mode-locked fiber lasers. *IEEE J. Sel. Top. Quantum Electron.*, 18(1):389, 2012.

[52] K Tamura, EP Ippen, HA Haus, and LE Nelson. 77-fs pulse generation from a stretched-pulse mode-locked all-fiber ring laser. *Opt. Lett.*, 18(13):1080–1082, 1993.

[53] Andy Chong, Joel Buckley, Will Renninger, and Frank Wise. All-normal-dispersion femtosecond fiber laser. *Opt. Express*, 14(21):10095, 2006.

[54] F. W. Wise. Fiber sources of femtosecond pulses in the mid-infrared. In *Proc. SPIE 10193, Ultrafast Bandgap Photonics II*, page 101930T, 2017.

[55] Y. Tang, L. G. Wright, K. Charan, T. Wang, C. Xu, and F. W. Wise. Generation of intense 100 fs solitons tunable from 2 to 4.3 μm in fluoride fiber. *Optica*, 3(9):948, 2016.

[56] F. Maes, V. Fortin, S. Poulain, M. Poulain, J.-Y. Carree, M. Bernier, and R. Vallée. Room-temperature fiber laser at 3.92 μm. *Optica*, 5(7):761–764, 2018.

[57] M. R. Majewski, R. I. Woodward, J.-Y. Carree, S. Poulain, M. Poulain, and S. D. Jackson. Emission beyond 4 μm and mid-infrared lasing in a dysprosium-doped indium fluoride (InF3) fiber. *Opt. Lett.*, 43(8):1926, 2018.

[58] Nicolas Caron, Martin Bernier, Dominic Faucher, and Réal Vallée. Understanding the fiber tip thermal runaway present in 3 μm fluoride glass fiber lasers. *Opt. Express*, 20(20):22188–94, 2012.

[59] Y. O. Aydin, F. Maes, V. Fortin, S. T. Bah, R. Vallée, and M. Bernier. Endcapping of high-power 3 µm fiber lasers. *Optics Express*, 27(15):20659, 2019.

[60] G. Stevens and T. Woodbridge. Mid-IR fused fiber couplers. *Proc. SPIE*, 9730:973007, 2016.

[61] E. C. Magi, L. B. Fu, H. C. Nguyen, M. R. E. Lamont, D. I. Yeom, and B. J. Eggleton. Enhanced Kerr nonlinearity in As 2 Se 3 chalcogenide fibre tapers with sub-wavelength diameter. *Opt. Express*, 15(16):10324, 2007.

[62] Dong-Il Yeom, E. C. Magi, M. R. E. Lamont, M. A. F. Roelens, L. Fu, and B. J. Eggleton. Low-threshold supercontinuum generation in highly nonlinear chalcogenide nanowires. *Opt. Lett.*, 33(7):660, 2008.

[63] Darren D. Hudson, Stephen A. Dekker, Eric C. Magi, Alexander C. Judge, Stuart D. Jackson, Enbang Li, J. S. Sanghera, L. B. Shaw, I. D. Aggarwal, and Benjamin J. Eggleton. Octave spanning supercontinuum in an As2S3 taper using ultra-low pump pulse energy. *Opt. Lett.*, 36(7):224–225, 2011.

[64] IRFlex: https://irflex.com/. 2019.

[65] Roberto Osellame, Giulio Cerullo, and Roberta Ramponi. *Femtosecond Laser Micromachining: Photonic and Microfluidic Devices in Transparent Materials*. 2012.

[66] Alexander Arriola, Sebabrata Mukherjee, Debaditya Choudhury, Lucas Labadie, and Robert R Thomson. Ultrafast laser inscription of mid-IR directional couplers for stellar interferometry. *Opt. Lett.*, 39(16):4820–2, 2014.

[67] G. Bharathan, D. D. Hudson, R. I. Woodward, S. D. Jackson, and A. Fuerbach. In-fiber polarizer based on a 45-degree tilted fluoride fiber Bragg grating for mid-infrared fiber laser technology. *OSA Contin.*, 1(1):56–63, 2018.

[68] D Strickland and G Mourou. Compression of amplified chirped optical pulses. *Opt. Commun.*, 56(3):219–221, 1985.

[69] R. I. Woodward, D. D. Hudson, A. Fuerbach, and S. D. Jackson. Generation of 70-fs pulses at 2.86 μm from a mid-infrared fiber laser. *Opt. Lett.*, 42(23):4893, 2017.

[70] Ian Coddington, Nathan Newbury, and William Swann. Dual-comb spectroscopy. *Optica*, 3(4):414, 2016.

[71] R. I. Woodward, M. R. Majewski, D. D. Hudson, and S. D. Jackson. Swept-wavelength mid-infrared fiber laser for real-time ammonia gas sensing. *APL Photonics*, 4:020801, 2019.

[72] Saeid Amini-Nik, Darren Kraemer, Michael L. Cowan, Keith Gunaratne, Puviindran Nadesan, Benjamin A. Alman, and R. J. Dwayne Miller. Ultrafast mid-IR laser scalpel: Protein signals of the fundamental limits to minimally invasive surgery. *PLoS One*, 5(9):1–6, 2010.